Electronic Supplementary Material (ESI) for Journal of Materials Chemistry A.

Aggregation-Induced Enhanced Photoluminescence in Magnetic Graphene Oxide Quantum dots as Fluorescence Probe for Arsenic (III) Sensing

Shabnam Pathan,[†] Misna Jalal,[†] Sanjay Prasad,[‡] Suryasarathi Bose *,[†]

[†]Department of Materials Engineering, Indian Institute of Science, Bangalore-560012, India

[‡] Inorganic and Physical Chemistry, Indian Institute of Science, Bangalore-560012, India

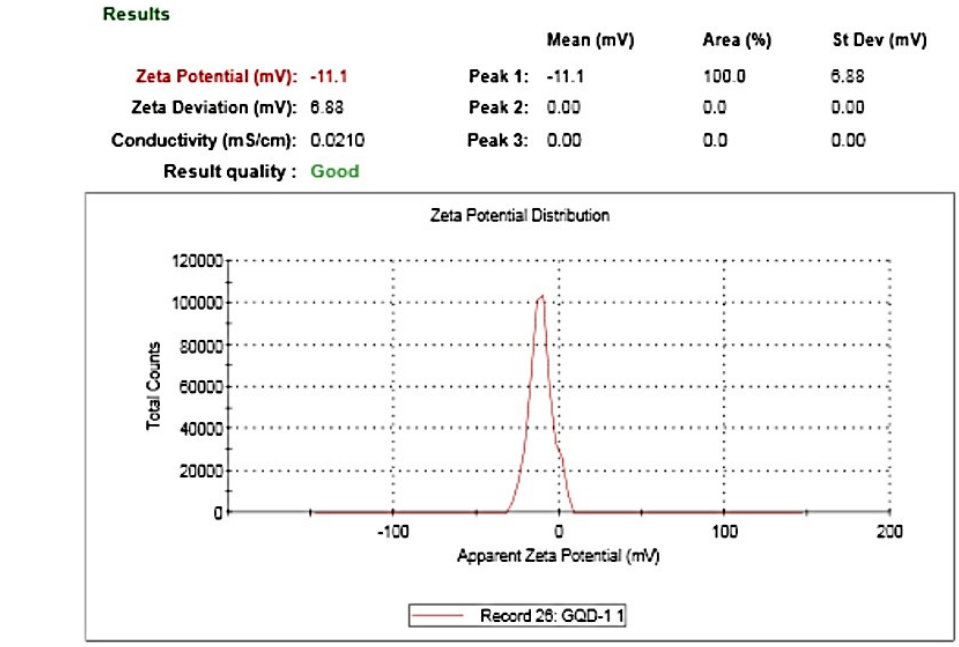

Figure S1 Zeta potential graph of GQDs

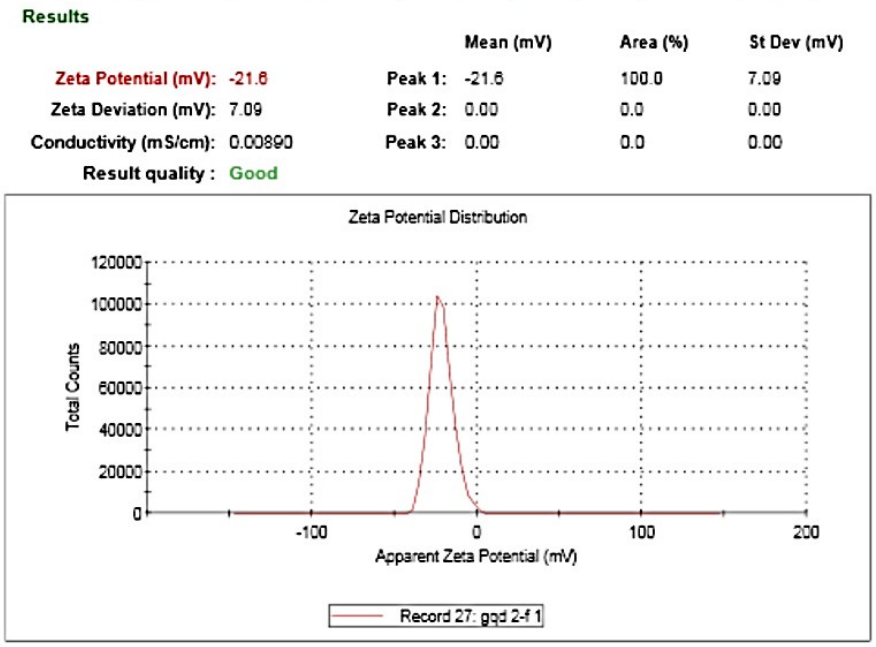

Figure S2 Zeta potential graph of Fe-GQDs

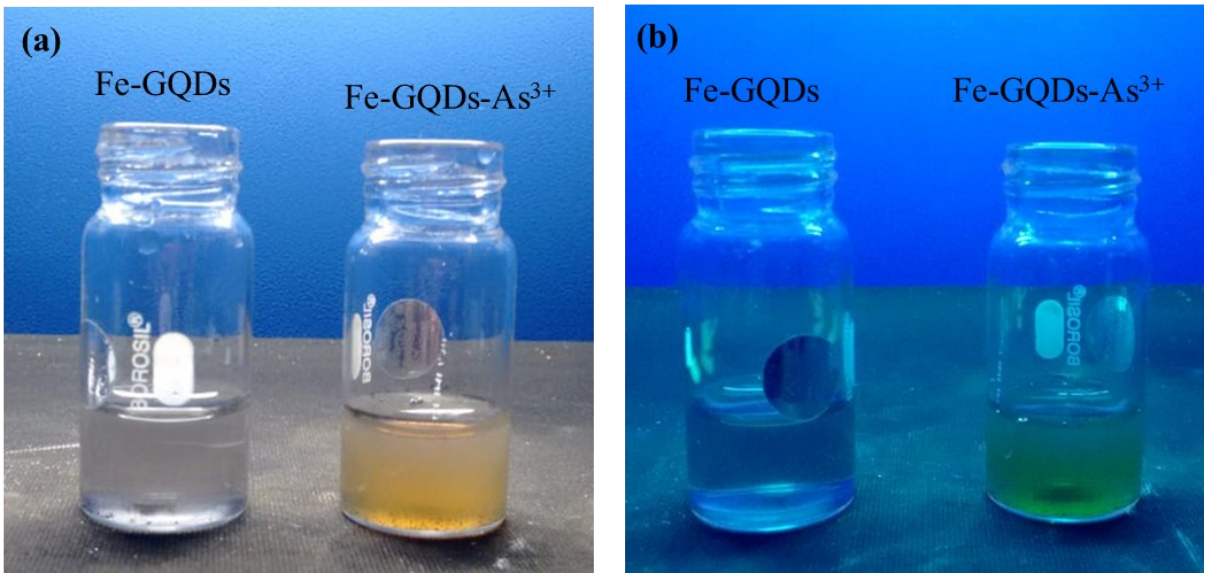

Figure S3. Digital photographs of Fe-GQDs and Fe-GQDs-As^{3+} (a) in white light (b) UV light

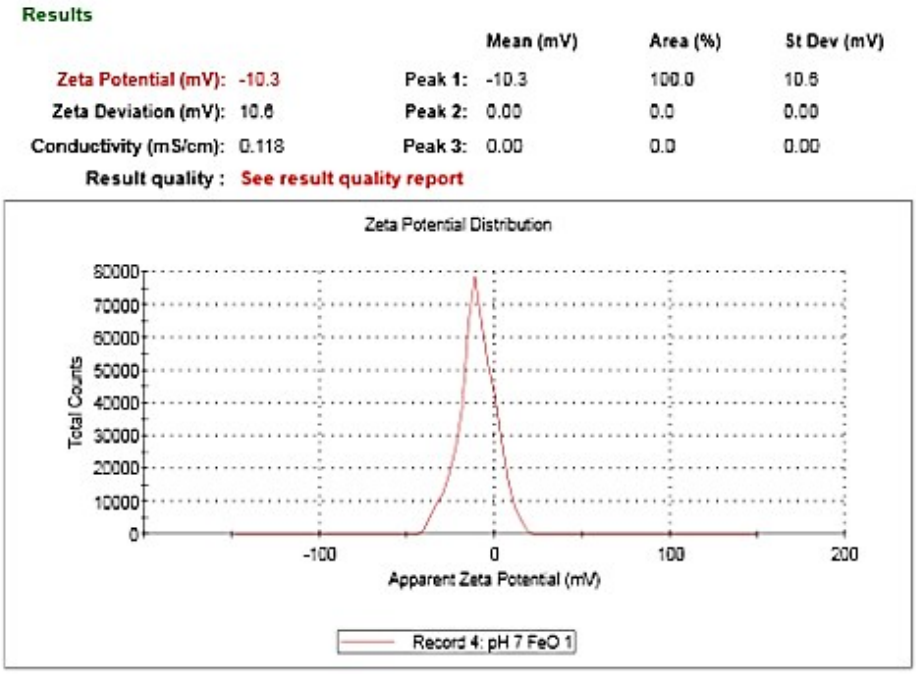

Figure S4 Zeta potential graph of Fe-GQDs at pH 7 after arsenic ion addition

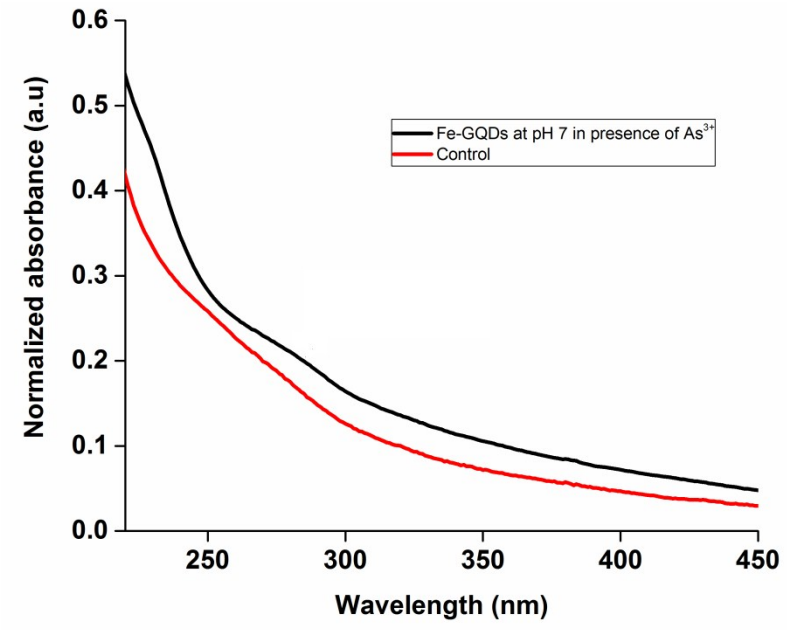

Figure S5 UV-visible absoprtion spectra of Fe-GQDs before and after arsenic addtion

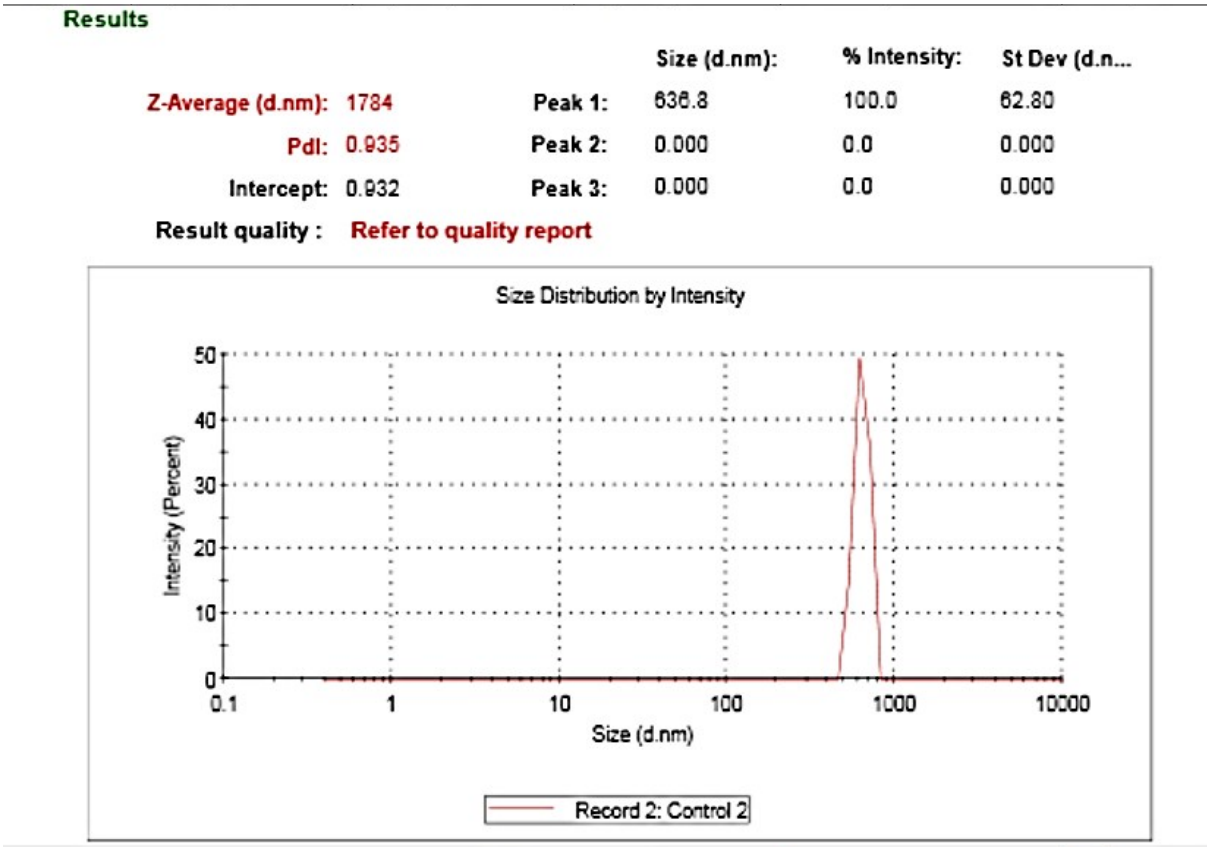

Figure S6 DLS graph of Fe-GQDs without As^{3+} ions

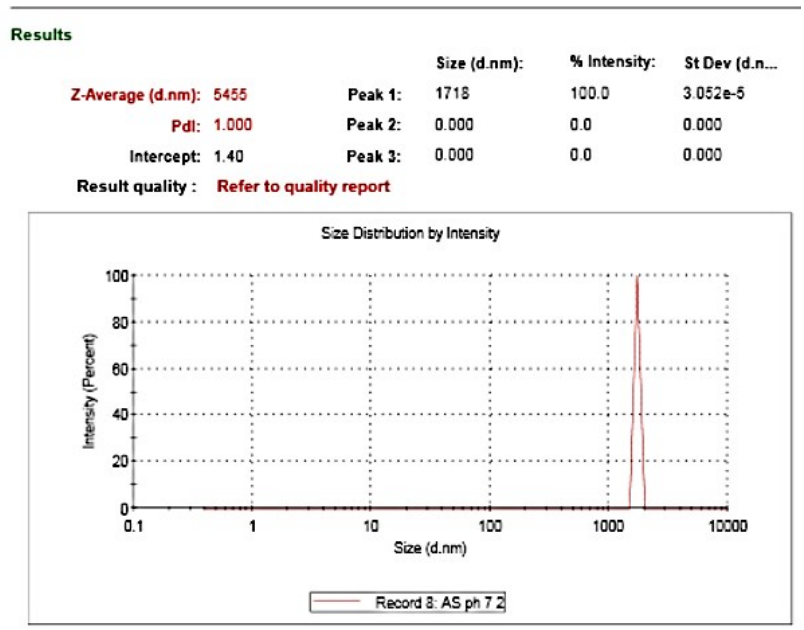

Figure S7 DLS graph of Fe-GQDs with As^{3+} ions at pH 7

Table S2 Photophysical parameters of Fe-GQDs before and after arsenic addition

Sample	τ_f (avg. ns)	χ^2
Fe-GQDs	4.0	1.35
Fe-GQDs-As^{3+}	6.02	1.27

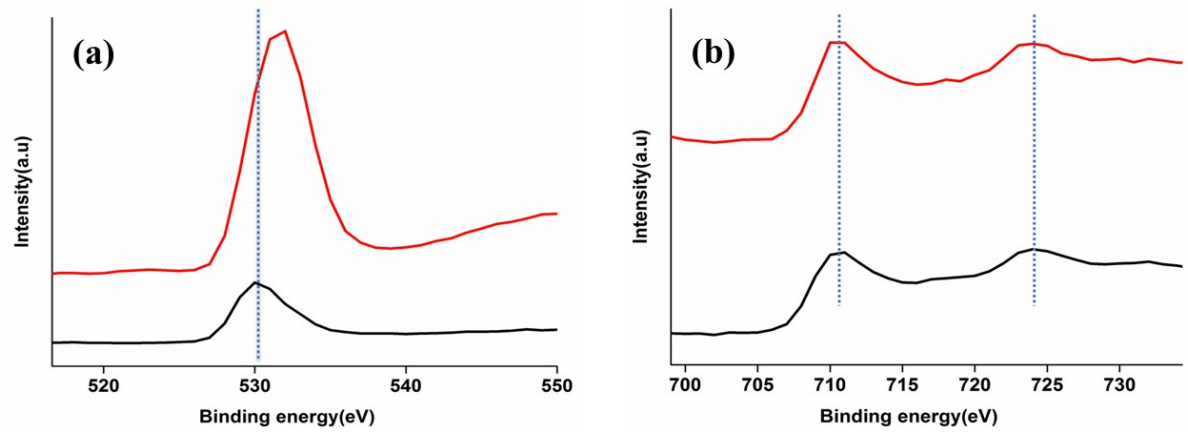

Figure S8 Enlarged view of O1s and Fe2p of Fe-GQDs after arsenic interaction

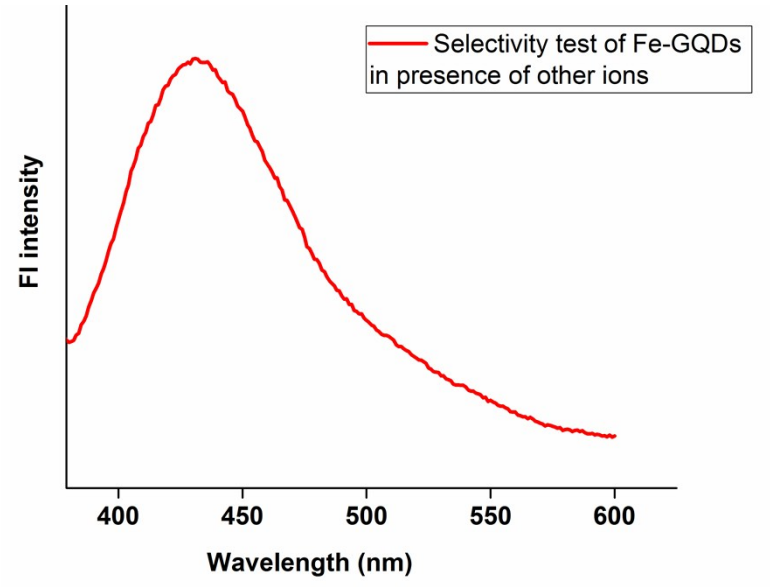

Figure S9 Interferring studies of Fe-GQDS in a mixture of other ions along with As^{3+} ions

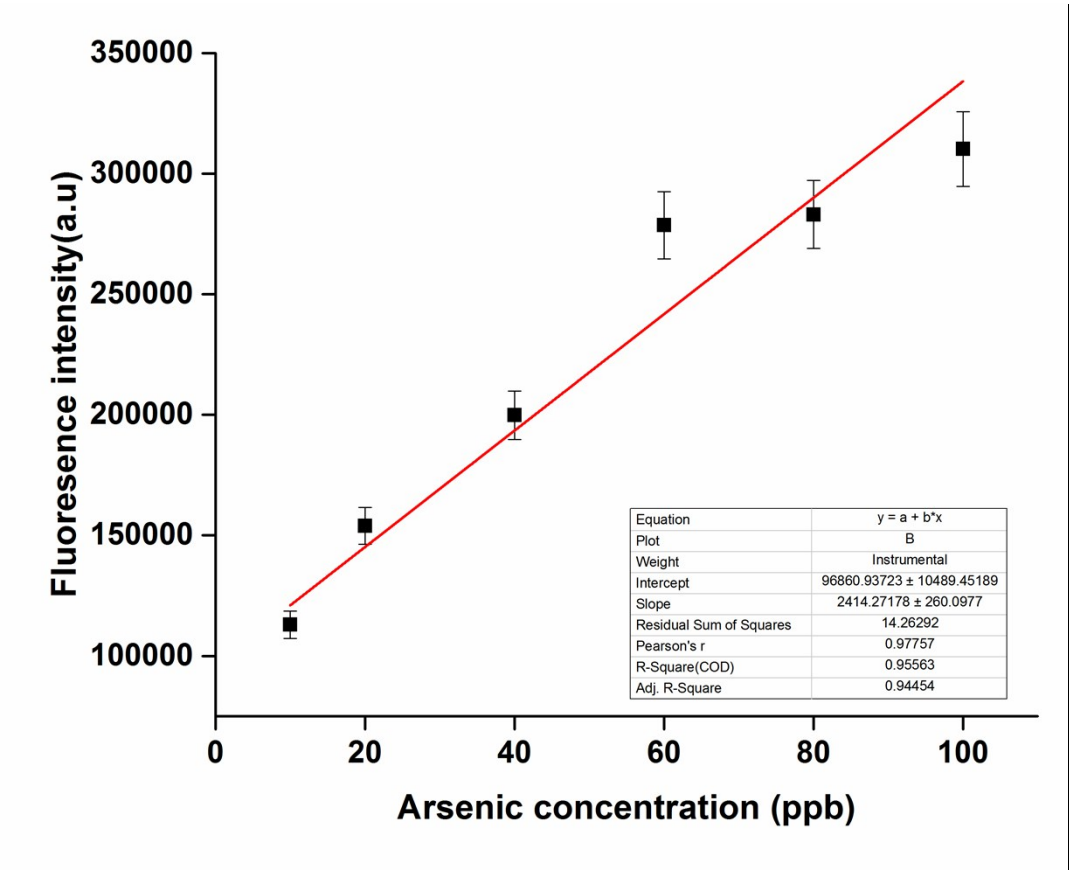

Figure S10 Linear graph showing fluorescence efficiency as a function of different concentrations of As^{3+} in Tap water

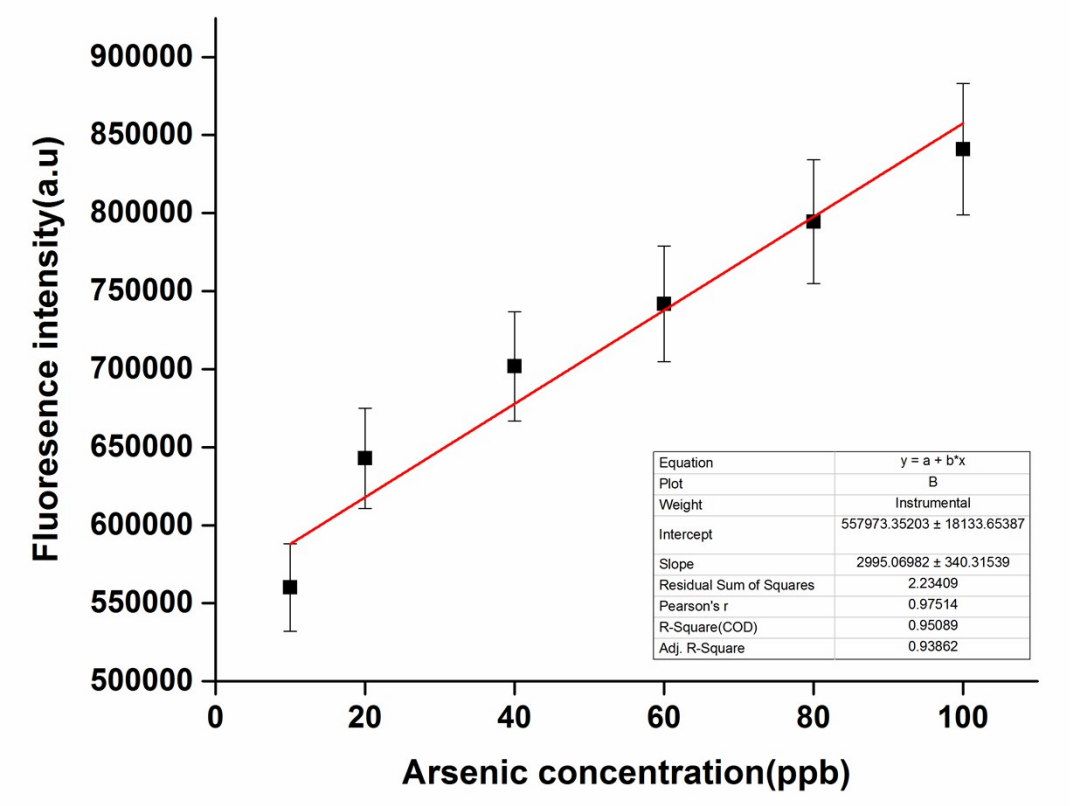

Figure S11. Linear graph showing fluorescence efficiency as a function of different concentrations of As^{3+} in recycled water

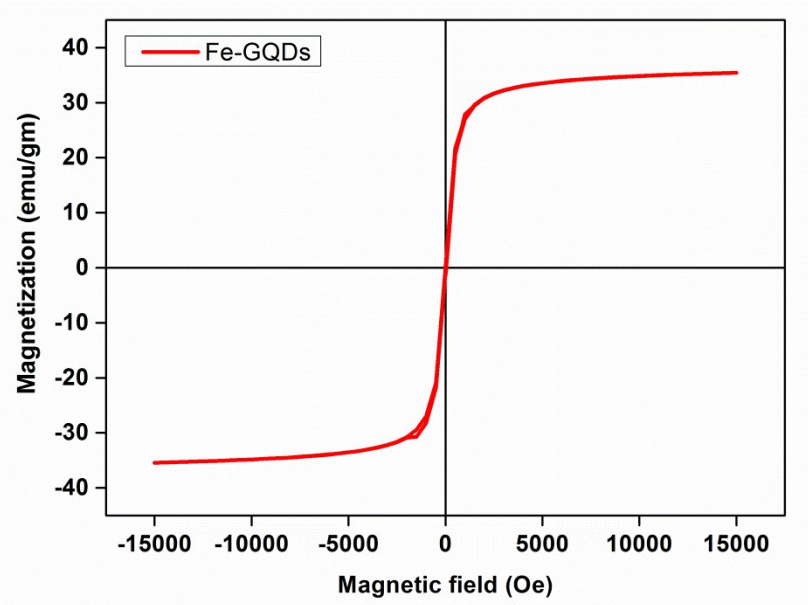

Figure S12 Magnetization curve of Fe-GQDs

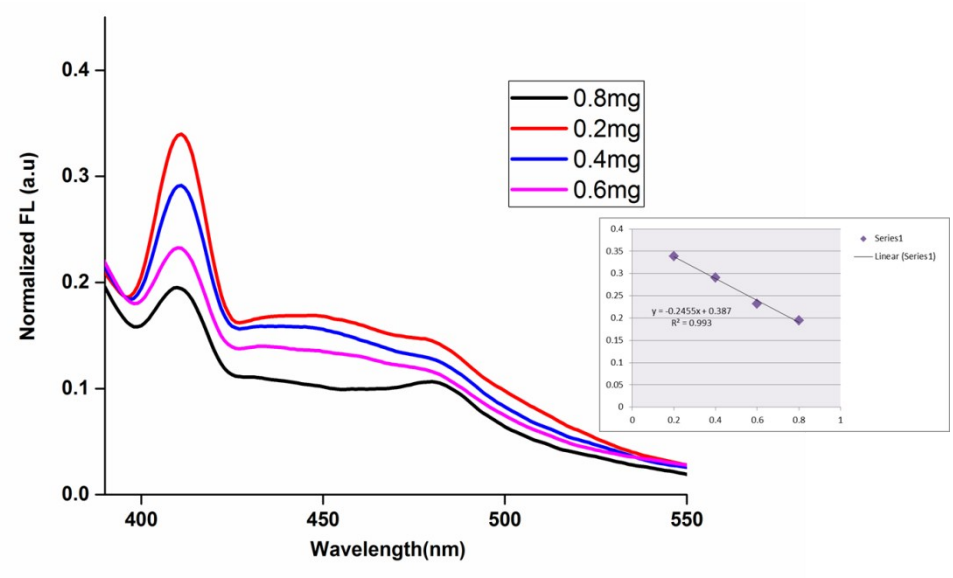

Figure S13 Concentration dependent FL emission spectra

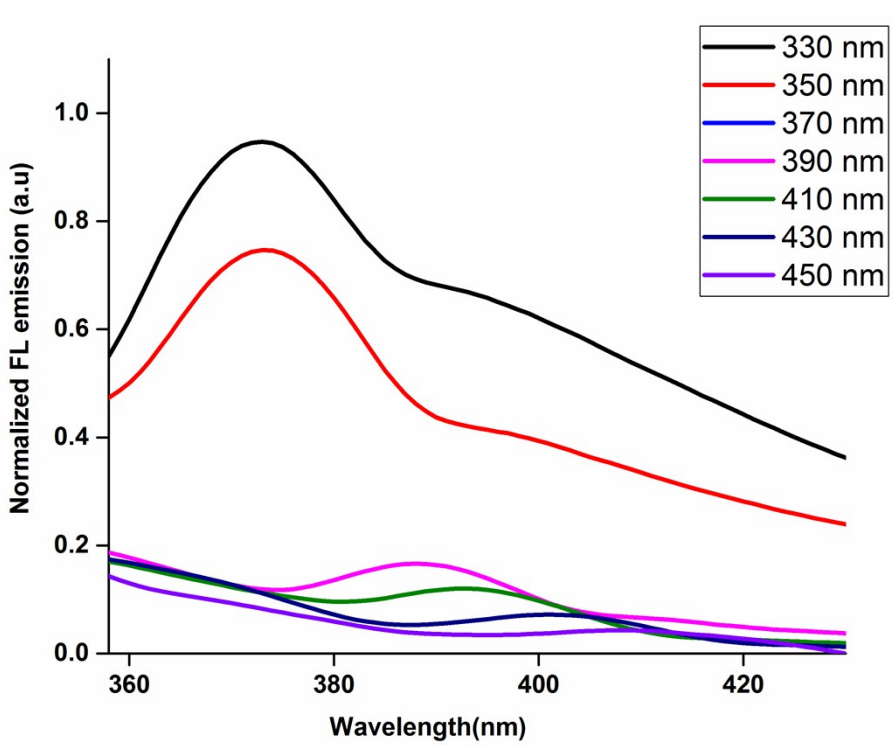

Figure S14 FL emission at different wavelength

Antibacterial study of Fe-GQDs

Reactive Oxygen Species (ROS) Quantification in E.coli cell

When bacterial cells are subjected to various environmental or chemical environments, it induces stresses on them. These stresses are in form of intracellular reactive oxygen species. A strong co-relation exists between these stresses and the bacterial reduction. [1-3] For this, the Fe-GQDs were incubated with 100 µL of E.coli culture for 2 h and DCFH-DA (dichlorodihydrofluorescein diacetate) dye was used to evaluate the generation of ROS. As evident from Figure S15a and S15b, no ROS was observed in control, however, significant green fluorescence is observed in Fe-GQDs treated bacterial cells. These ROS species interacts and disrupt the cell integrity of the bacterial cell and finally led to the cell death.

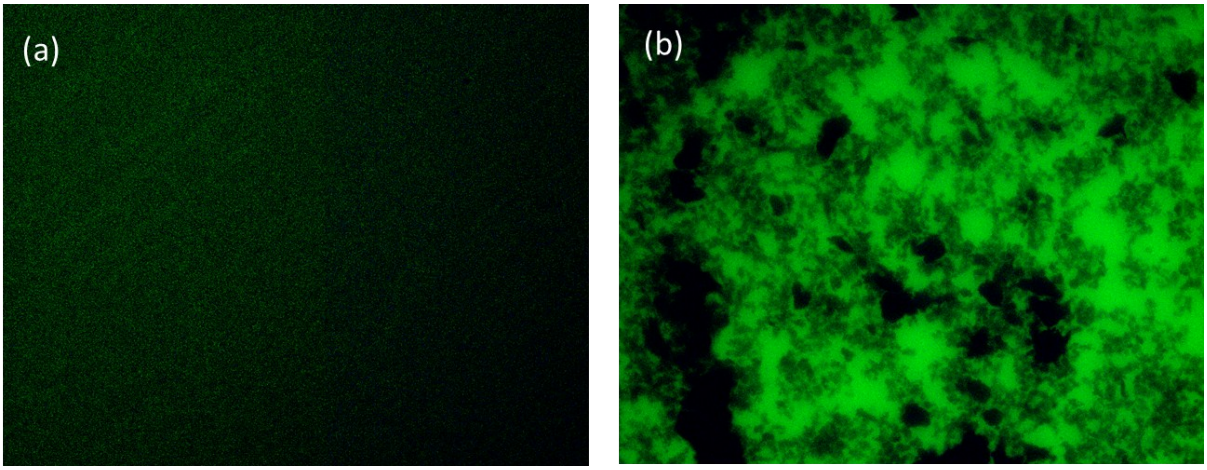

Figure S15 ROS generation (a) in the absence and (b) in the presence of Fe-GQDs

Further, we assessed the reactive oxygen species generation (in cps) as a function of different time periods (5 min, 10 min and 15 min) in presence of UV light. It was observed that the level of ROS generation (Figure S16) was more for Fe-GQDs as compared to the control sample upon UV irradiation. Additional, a significant amount of ROS was generated after 10 mins which attained saturation after 15 mins. An intracellular ROS is a preliminary marker for bacterial stress and a potential indicator of bacterial cell death.[4] From the obtained results

we hypothesize that the prepared Fe-GQDs nanoparticles are antibacterial in nature. The facile and quick response in terms of intense oxygen species generation from Fe-GQDs can be ascribed from the synergistic effect of Fe_3O_4 nanoparticles and GQDs. Herein, we assume Fe-GQD based nanoparticles in *E.coli* suspension mediated a series of different redox reactions via Fenton's chemistry which generates hydroxyl radicals. This effect was aggravated by GQDs. Absorption of light in semiconductor GQDs led to the generation of electron-hole pair, which later reacted with the surrounding molecular oxygen or water to form various oxygen moieties. Further, some of the trapped electrons with the adsorbed oxygen molecules would have formed $O^{2\bullet-}$ and holes would have reacted with the H_2O molecules forming $^{\bullet}OH$. [5-8]These radicals concern are toxic to bacterial cells hence these particles can effectively remediate bacterial contaminated water besides removing As^{3+} ions.

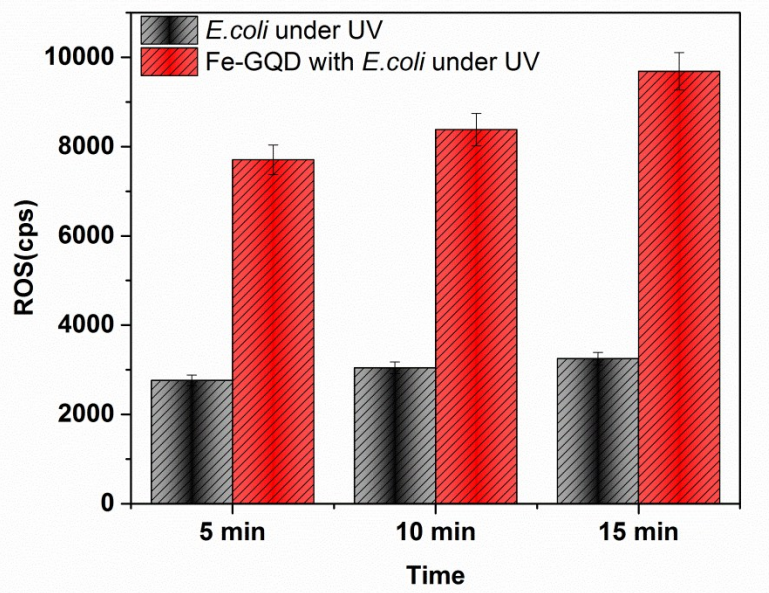

Figure S16 Photo induced ROS production for Fe-GQDs and control

References:

(1) Samantaray, P. K.; Madras, G.; Bose, S. PVDF/PBSA membranes with strongly coupled phosphonium derivatives and graphene oxide on the surface towards antibacterial and antifouling activities. *Journal of Membrane Science* **2018,** *548*, 203-214.
(2) Samantaray, P. K.; Baloda, S.; Madras, G.; Bose, S. A designer membrane tool-box with a mixed metal organic framework and RAFT-synthesized antibacterial polymer perform in tandem towards desalination, antifouling and heavy metal exclusion. *Journal of Materials Chemistry A* **2018,** *6* (34), 16664-16679.
(3) Samantaray, P. K.; Madras, G.; Bose, S. Water Remediation Aided by a Graphene-Oxide-Anchored Metal Organic Framework through Pore-and Charge-Based Sieving of Ions. *ACS Sustainable Chemistry & Engineering* **2018,** *7* (1), 1580-1590.
(4) Samantaray, P. K.; Madras, G.; Bose, S. Antibacterial and Antibiofouling Polymeric Membranes through Immobilization of Pyridine Derivative Leading to ROS Generation and Loss in Bacterial Membrane Integrity. *ChemistrySelect* **2017,** *2* (26), 7965-7974.
(5) Arakha, M.; Pal, S.; Samantarrai, D.; Panigrahi, T. K.; Mallick, B. C.; Pramanik, K.; Mallick, B.; Jha, S. Antimicrobial activity of iron oxide nanoparticle upon modulation of nanoparticle-bacteria interface. *Scientific reports* **2015,** *5*, 14813.
(6) Chong, Y.; Ge, C.; Fang, G.; Tian, X.; Ma, X.; Wen, T.; Wamer, W. G.; Chen, C.; Chai, Z.; Yin, J.-J. Crossover between anti-and pro-oxidant activities of graphene quantum dots in the absence or presence of light. *ACS nano* **2016,** *10* (9), 8690-8699.
(7) Furube, A.; Tamaki, Y.; Murai, M.; Hara, K.; Katoh, R.; Tachiya, M. In *Femtosecond visible-to-IR spectroscopy of TiO 2 nanocrystalline films: Dynamics of UV-generated charge carrier relaxation at different excitation wavelengths*, Physical Chemistry of Interfaces and Nanomaterials Vi, International Society for Optics and Photonics: 2007; p 66430J.
(8) Bose, S.; Samantaray, P. Cationic biocide anchored graphene oxide-based membranes for water purification. *Proceedings of the Indian National Science Academy* **2018,** *84* (3), 669-679.